The International Journal of Advanced Manufacturing Technology (2022) 120:6515–6529
https://doi.org/10.1007/s00170-022-09094-3

ORIGINAL ARTICLE

Influence of welding parameters on grain size, HAZ and degree of dilution of 6063-T5 alloy: optimization through the Taguchi method of the GMAW process

José L. Meseguer-Valdenebro[1] · Eusebio Martínez-Conesa[1] · Antonio Portoles[2]

Received: 6 January 2022 / Accepted: 21 March 2022 / Published online: 12 April 2022

Abstract
The aim of this work is to design experiments using Taguchi's method that determine the influence of welding parameters on the grain size, heat-affected zone and degree of dilution of the 6063-T5 alloy. The welding process used is GMAW, and the welding parameters are the power, welding speed and bevel spacing. The study of the influence of these welding parameters on the measurements made during welding (which are the size of the heat-affected zone, the degree of dilution and the grain size) allows one to determine the quality of the joint. In addition, the welding parameter that most influences the minimisation of these three measurements will be determined.

Keywords Weld · Aluminium · HAZ · Taguchi · Optimization

1 Introduction

Aluminium alloys are characterised by harder or softer mechanical properties depending on the quality and quantity of the alloying elements that are present in the aluminium matrix [1]. These alloying elements can be lost due to the thermal input received during welding [2, 3]. On the other hand, the size of the grain in the alloy also determines the mechanical properties of the aluminium alloy, which is more resistant as the size of the grain decreases. Finally, the size of the HAZ is also relevant: the smaller its size, the better the properties of the weld joint, without taking into account the effect of residual stresses. The grain size [4] is determined by microscopic analysis using comparative charts according to the ASTM E112 [5] and NF ISO 643 [6] standards. There are computer programs that, using the microstructure of a weld, can estimate the size of the grains from polarisation micrographs and image orientation [7]. There are other programs that can determine the grain size from statistical analysis, specifically by estimating the grain size from the parameters of the grain [8]. These programs, which are used in specialised metallurgy laboratories and detect the microstructure and grain size of welds, consist of powerful intelligent algorithms that determine the structure to be analysed through values that they compare with a set of standard samples. The main advantage of these programs is that a large number of metallographic replicas can be rapidly analysed. The downside is that the image quality, sample preparation, polish quality, etc., influence the results. This technique can be used when many metallographic replicas are made, and the preparation procedure of the metallographic sample to be analysed is controlled.

Arc welding processes using GTAW for non-ferrous alloys have been substantially improved, resulting in high-quality microstructures [9–11].

The dilution between the filler material and the base material is defined as the ratio of molten base metal to the total amount of molten metal [12]. The dilution is expressed by the following expression:

$$\text{Dilution } (\%) = \frac{\text{Molten base metal}}{\text{Total molten metal}} \quad (1)$$

✉ Eusebio Martínez-Conesa
Eusebio.martinez@upct.es

José L. Meseguer-Valdenebro
jlmeseguer507@gmail.com

[1] Faculty of Architecture and Building Engineering, Universidad Politécnica de Cartagena, Cartagena, Spain

[2] Department of Applied Physics and Materials Engineering, ETSII, Technical University of Madrid, C/José Gutiérrez Abascal St, 2, 28006 Madrid, Spain

Table 1 Chemical composition of base metal

Si	Fe	Cu	Mn	Mg	Cr	Zn	Ti
0.20–0.60	0.35	0.10	0.45–0.90	0.45–0.90	0.10	0.10	0.10

The dilution is proportional to the thermal input of the heat source [13, 14], that is, the greater the thermal input, the greater the dilution [15]. In the present work, both the relationship between the thermal input and the dilution calculated for the weld bead and the relationship between the molten base material and the total amount of molten material are analysed. The lower the dilution, the lower the presence of base material in the weld bead and the better the quality of the weld bead.

Classical experimental design aims to identify the factors that affect the mean response and their influence on a target value. The advantage of using Taguchi experimental design instead is that it reduces the variability in the deviation from the mean target value [16–21].

The robust parameter design of Taguchi methods (orthogonal matrices) allows the influence of the factors to be analysed using just a few experiments. Taguchi's experiment designs are balanced; that is, no factor is analysed independently of the others. Accordingly, it is sufficient to perform nine experiments to evaluate the size of the weld grain, the size of the HAZ and the dilution of the filler material.

There are various studies that have performed the optimisation of welding processes using Taguchi methods. Several studies optimised the weld bead based on the electrical parameters of the source [22–24]. There is also an optimisation study that evaluated the welding thermal cycle [25]. All these studies were carried out using the GMAW process [26–29].

The present work aims to study the effect of welding parameters, that is, the power (P), welding speed (Vs) and edge separation (Sp), on the grain size, HAZ size and dilution of the weld bead.

2 Experimental procedure

In a previous work [22], the weld that is the focus of the current paper was evaluated by determining the influence that the aforementioned parameters have on the geometry of the weld bead. In [22], which was written by the authors of this paper, the following is indicated.

Table 2 Chemical composition of filler metal

Mn	Si	Ti	Cu	Mg	Zn	Be	Fe
0.05	0.25	0.06	0.10	4.5	0.10	0.0008	0.4

Table 3 Factor levels

Level	*P* (W)	*Vs* (mm/s)	*Sp* (mm)
1	1557	11.5	0.0
2	1673	12.25	1.0
3	1744	13	1.2

The experimental procedure is carried out with a robot welding arm (brand – ABB, model – IR 1400), as shown in Fig. 1a. The robotic arm has six degrees of freedom of movement, and a system controls the welding parameters. The welding robot has a high precision, which guarantees the correct finish of the joint. The elements to be joined are nine tubes that each has an outside diameter of 50 mm, a thickness of 2 mm and a length of 150 mm; they have been cut longitudinally and subsequently joined by a welding bead. To be able to longitudinally connect the parts of the tube, a carbon steel tool was designed to support the two parts of the aluminium tube before they are welded. This tool is shown in Fig. 1b.

Aluminium 6063-T5 is usually supplied in the form of a tube and not in the form of sheets [20]. The filler metal used is ER-5356, which is very suitable for welding 6063-T5 [30]. The diameter of the wire used is 1 mm, and the protective gas is 99% argon. The type of transfer used by the welding process is short arc transfer [4, 29, 31]. The chemical compositions of the base metal and the filler metal are given in Tables 1 and 2, respectively.

2.1 Design of experiments

Three variables with three levels each were used to develop nine welding experiments according to the Taguchi method with an L9 orthogonal array. Table 3 shows the three variables used: the power (P), welding speed (Vs) and edge separation (Sp).

Three factorial levels arranged in ascending order were selected. For the power, 1557 W represents the minimum value of the power used in the experiment, 1673 W

Table 4 Matrix of experiments

Experiment no.	*P* (W)	*Vs* (mm/s)	*Sp* (mm)
1	1557	11.5	0.0
2	1557	12.25	1.0
3	1557	13.0	1.2
4	1673	11.5	1.0
5	1673	12.25	1.2
6	1673	13.0	0.0
7	1744	11.5	1.2
8	1744	12.25	0.0
9	1744	13.0	1.0

Table 5 Values of intensity and voltage used to obtain each power value

Power (W)	Intensity (A)	Voltage (V)
1557	90	17.3
1673	94	17.8
1744	98	17.8

represents the intermediate value of the power used in the experiment, and 1744 W represents the maximum value of the power used in the experiment. In the same way, for the welding speed and the separation of the plate edges, the value of the first level corresponds to the minimum value of the variable, the value of the second level corresponds to the intermediate value of the variable, and the value of the third level corresponds to the highest value of the variable [22].

To determine the matrix of nine experiments using Taguchi's method, the statistical software Minitab [32] was used. Table 4 shows the nine experiments determined using the Taguchi methodology. The power is obtained by multiplying the intensity by the voltage. Table 5 shows the intensity and voltage values used to obtain the three power values used in the experimental design.

3 Discussion of results

Figure 2 shows the nine welds corresponding to each of the experiments carried out according to Table 4. The welds have been polished with different grain sizes which makes it sound like 'grain sizes' were used to polish the welds, as indicated in [22].

Table 6 Grain size values obtained in the HAZ

Experiment no.	Grain G index	Number of grains
1	4	16
2	4	16
3	3.2	12
4	5.1	23
5	5.2	24
6	4	16
7	2	8
8	3.6	14
9	4.4	18

In reference [33], the effect of kind of gas on the appearance of defects that are showed in these welds is discussed. The main cause for which defects appear is because argon gas is used and not helium gas as is indicated in reference [33]. When argon is used as protection gas, the defects shown in Fig. 2 are more likely to appear. If helium gas is used, the probability of these defects appearing is less.

3.1 Macrographs of the nine experiments performed

To measure the grain size, Grani software is used. It allows the 'G' index to be calculated with precision according to the standards ASTM E112 [5] and ISO 643 [6]. A complete

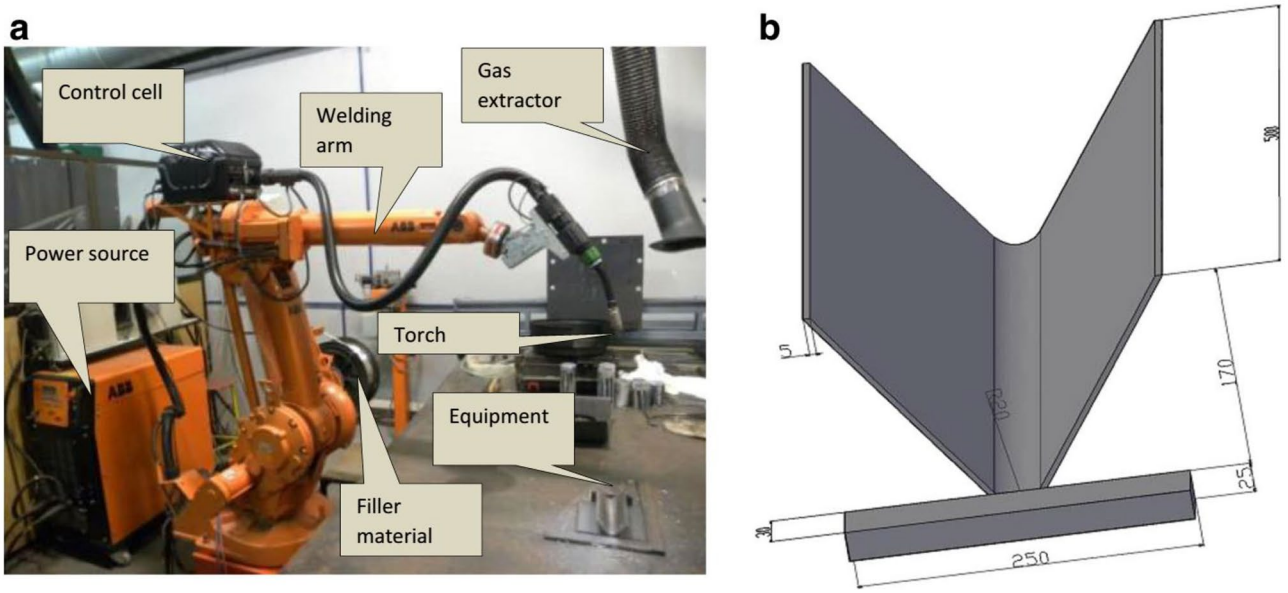

Fig. 1 (**a**) Photograph of the welding robot with the GMAW torch installed. (**b**) Tool used in the welding of the aluminium tube [22]

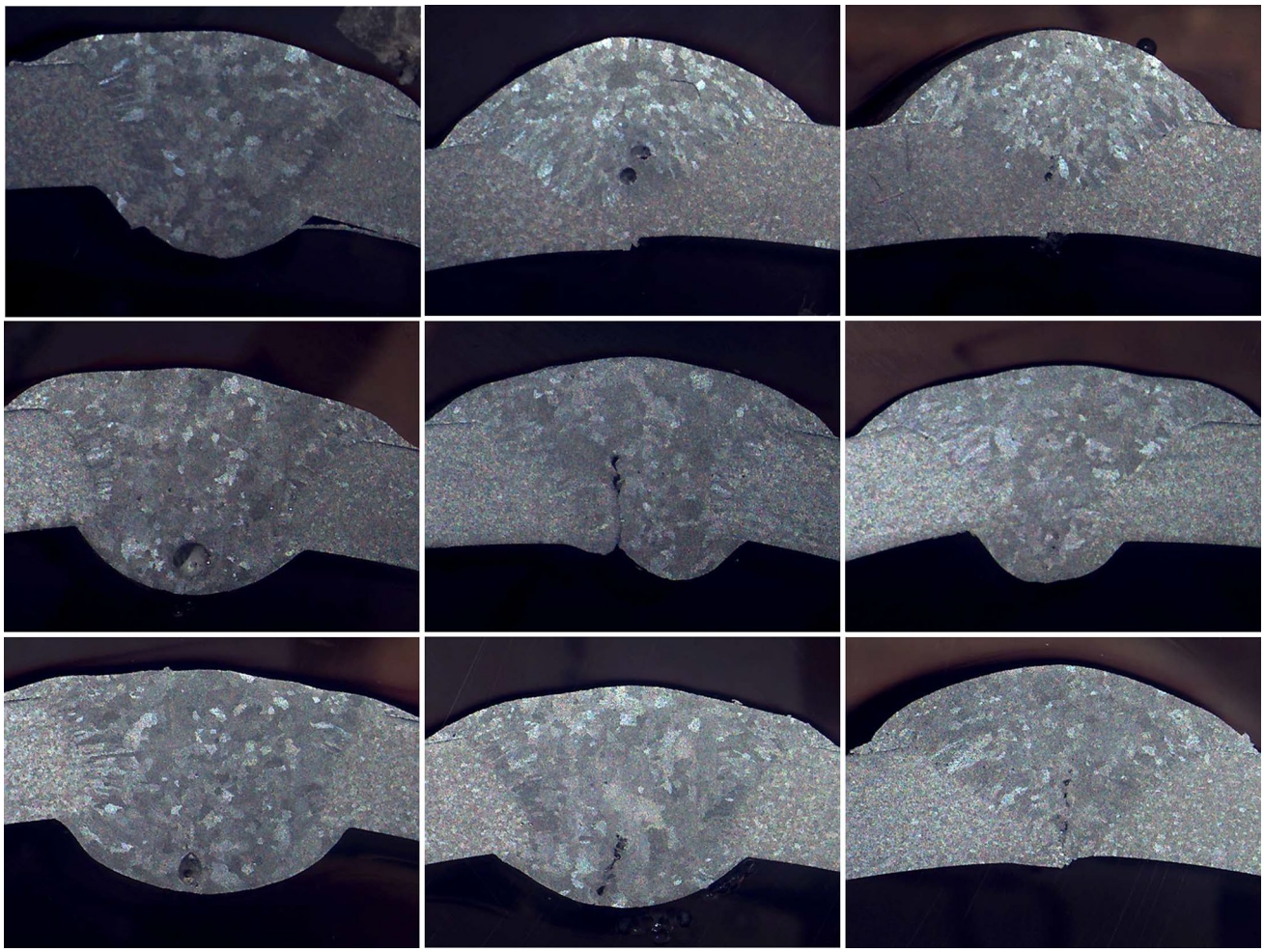

Fig. 2 Macrographs of the nine experiments performed

set of measurements is performed for each of the nine experiments using the Grani software.

On the macrograph, the grain size is measured in the thermally affected area, that is, in the HAZ. For each experiment, the G index of the grain and the number of grains are measured (Table 6). The Grani program uses the Hilliard method [23, 24] to determine these values. Figure 3 shows the measurements made in each experiment. A red circle marks the area where the grain's G index and the number of grains were measured.

Figure 4 represents the relationship between the G index of the ASTM standard and the number of grains identified by the Grani program. Therefore, the grain size is evaluated and not the letter number since the relationship is the same.

To evaluate the effect of each of the variables on the number of grains, the following multivariate linear regression equation is obtained:

$$\text{Number of grains} = 20.3 - 0.0011 \cdot P, W - 0.22 \cdot Vs,\ \text{mm/s} + 0.81 \cdot Sp,\ \text{mm} \quad (2)$$

In the analysis of variance in Table 7, the influence of each of the variables on the grain size is determined. The three P-values shown are large, that is, they indicate that these variables do not have a significant influence on the number of grains in the aluminium weld. Therefore, these three variables do not affect the number of grains in the weld.

In accordance with the above, the effect of the three main variables on the number of grains is not further analysed because they have not influenced the number of grains.

Table 7 Analysis of variance (ANOVA)

Source	DF	Adj SS	Adj MS	*F*-value	*P*-value
Regression	3	1.845	0.6149	0.02	0.997
P, *W*	1	0.065	0.0651	0.00	0.969
Vs, mm/s	1	0.167	0.1667	0.00	0.951
Sp, mm	1	1.613	1.6129	0.04	0.848
Error	5	198.155	39.6311		
Total	8	200.000			

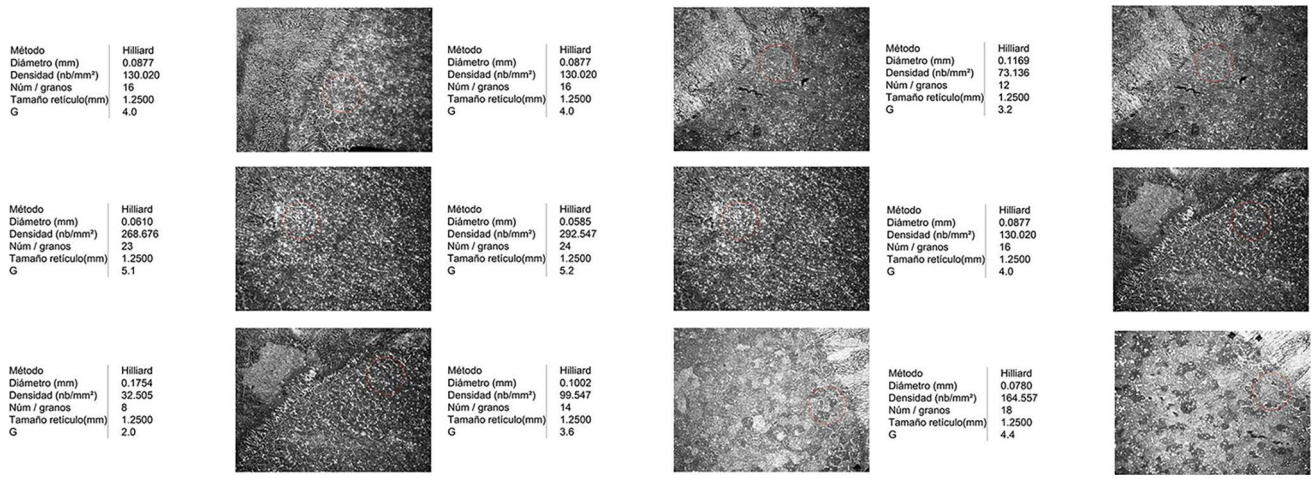

Fig. 3 Micrographs of measured grain sizes

3.2 Size of the HAZ in each experiment performed

The size of the HAZ of each weld is measured using a profile meter that shows the test tubes used in each experiment on which the size of the HAZ is measured using the profile meter that is showed in reference [22].

Figure 5 shows the micrographs of the HAZ made for each of the joints.

In each of the experiments, the size of the HAZ is measured; it is shown in red on each of the micrographs. The following HAZ values are obtained.

To evaluate the effect of each of the variables on the size of the HAZ, the following multivariate linear regression equation is obtained:

$$\text{Size of HAZ} = -1.30 + 0.001831 \cdot P, W - 0.0778 \cdot Vs,\ \text{mm/s} + 0.1495 \cdot Sp,\ \text{mm} \tag{3}$$

Equation 3 has an adjusted R2 value of 51.87%, which is not close to 95%.

Figure 6 shows the trend of each of the variables versus the size of the HAZ.

Table 9 shows the influence of each of the variables on the size of the HAZ as determined by the analysis of variance. The three P-values shown are small, that is, they indicate that these variables have a significant influence on the size of the HAZ of the aluminium weld. Therefore, these three variables significantly affect the size of the HAZ of the weld.

The variable that has the most influence is power (P); it is followed by the edge separation (Sp), which in turn

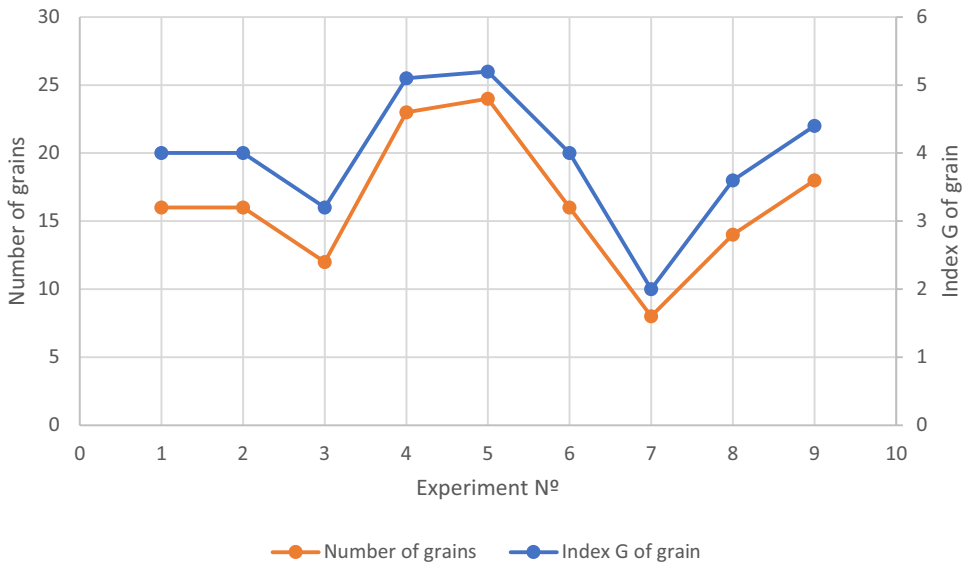

Fig. 4 Relationship between the G index and grain size

Table 8 HAZ size for each experiment

Experiment no.	Size of HAZ (mm)
1	0.64
2	0.65
3	0.76
4	0.89
5	1.17
6	0.84
7	1.27
8	0.92
9	0.85

is followed by the welding speed (Vs). Figure 7 shows the effect of each of the variables on the size of the HAZ.

From Fig. 7, the specific contributions of each of the variables to the size of the HAZ are obtained: P = 53%, Sp = 29% and Vs = 18%.

3.3 Dilution obtained in each of the experiments performed

Figure 8 shows the area of dilution in the weld bead (area enclosed by a red outline). As shown in Eq. (1), the dilution ratio is determined by dividing the amount of molten base metal by the total amount of molten metal.

Figure 8 shows the dilution values (%), weld bead area and molten base metal area. The area of the weld bead was measured in [22] using a profile meter.

3.3.1 Determination of the degree of dilution

The area of the molten base metal is determined from the CAD representation of the weld joint using the profile gauge and the initial geometry of the tubular profile before it is welded. The bead is superimposed on the tube geometry, and the amount of molten base metal found in the weld metal is obtained. Figure 9 represents the weld bead and base metal for each of the experiments. The edge separation, Sp, is considered in determining the degree of dilution.

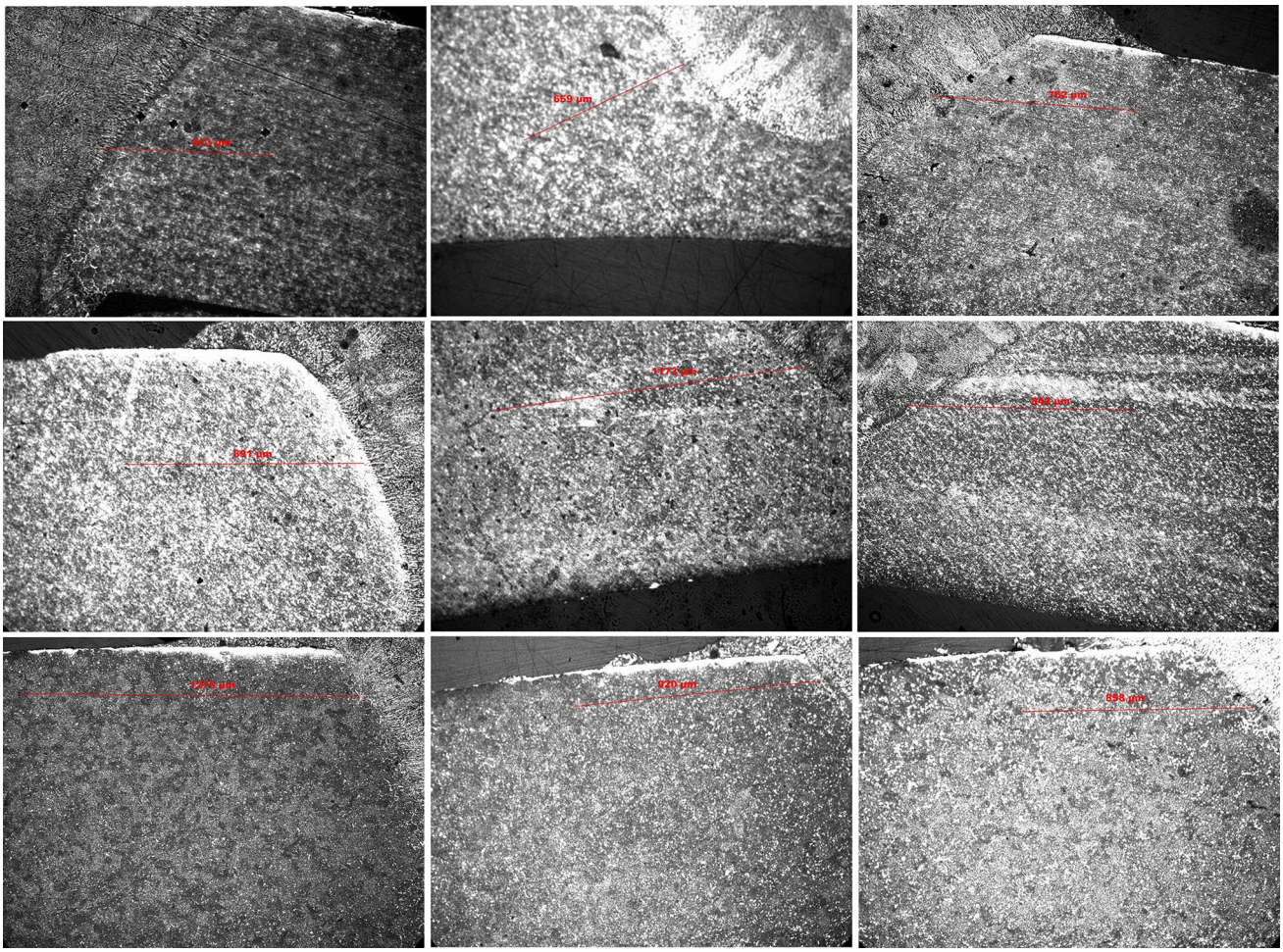

Fig. 5 Micrographs of the HAZ

Table 9 Analysis of variance (ANOVA)

Source	DF	Adj SS	Adj MS	*F*-value	*P*-value
Regression	3	0.25504	0.08501	3.87	0.089
P, *W*	1	0.17923	0.17923	8.17	0.035
Vs, mm/s	1	0.02042	0.02042	0.93	0.379
Sp, mm	1	0.05540	0.05540	2.52	0.173
Error	5	0.10971	0.02194		
Total	8	0.36476			

To evaluate the effect of each of the variables on the dilution of the base metal by the weld metal, the following multivariate linear regression equation is obtained:

$$\text{Dilution} = 0.207 + 0.000834 \cdot P, W - 0.0889 \cdot Vs, \frac{\text{mm}}{\text{s}} - 0.1616 \cdot Sp, \text{ mm} \quad (4)$$

The fit of Eq. 4 has an adjusted R2 value of 70.09%, which is acceptable because it is close to 100% and because the P-values of Table 11 are low. This is explained in the Minitab guide [32].

Figure 10 represents the trend of each of the welding variables versus the dilution in the weld bead. As the power increases, the dilution in the weld bead increases, and as both Vs and Sp decrease, the dilution in the weld bead decreases.

In the analysis of variance in Table 11, the influence of each of the variables on the degree of dilution is determined. The three P-values shown are small, that is, they indicate that these variables have a significant influence on the degree of dilution in the weld bead. Therefore, these three variables significantly affect the degree of dilution in the weld bead.

In Fig. 11, the influence of each of the variables on the degree of dilution is presented. The variable that has the most influence is the edge separation, Sp, followed by the power, P, which in turn is followed by the welding speed, Vs.

From Fig. 11, the specific contribution of each of the variables (P 32%; Sp 42%; Vs 27%) on the dilution of the base metal in the weld bead is obtained.

4 Optimisation of results

After the experiments are carried out and the grain size, the size of the HAZ and the dilution in the weld are measured, the analysis of variance is used to determine the influence of the welding parameters, P, Vs and Sp, which are then optimised using the Taguchi method and the statistical program Minitab [27]. The criterion to be used in the Taguchi optimisation is 'the smaller the better' for both the degree of dilution and the size of the HAZ.

The grain size will not be analysed because, as indicated above, there is no relationship between the welding variables and the grain size; therefore, an evaluation of the grain size is not performed.

4.1 Taguchi optimisation

Methodology of Taguchi is a suitable one in the optimization of welding processes as indicated in reference [34]. According to this, it is considered that the methodology of Taguchi is suitable for the optimization of welding processes.

The noise signal ratio (S/N) for the case 'the smaller the better' is determined as follows.

The S/N ratio is defined as

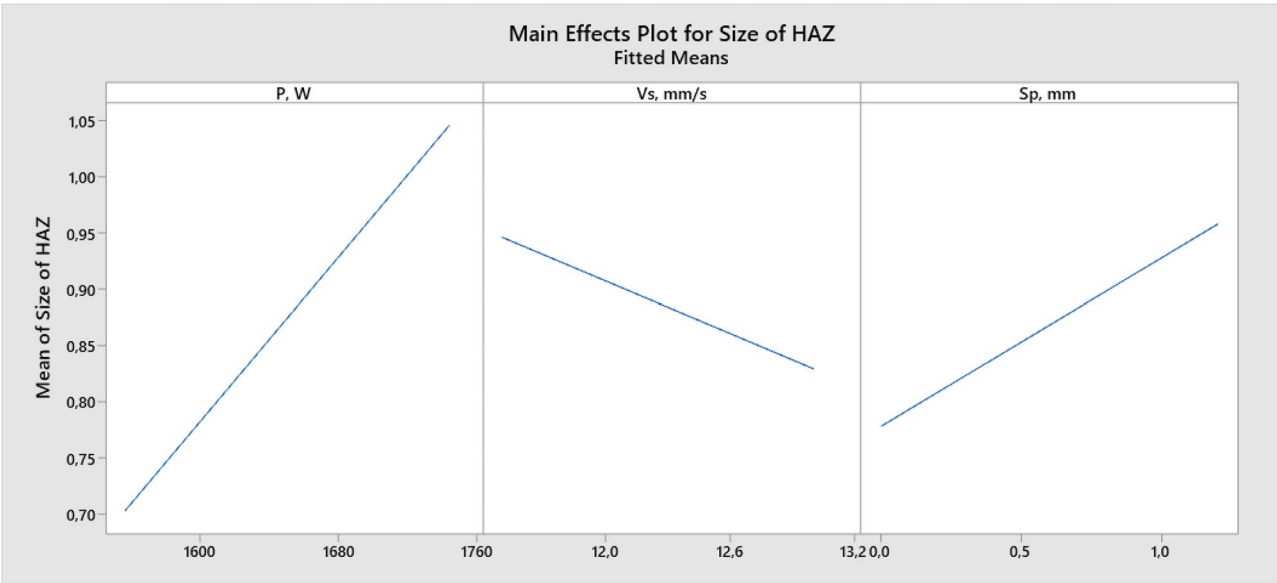

Fig. 6 Representation of the effect of each of the variables on the size of the HAZ

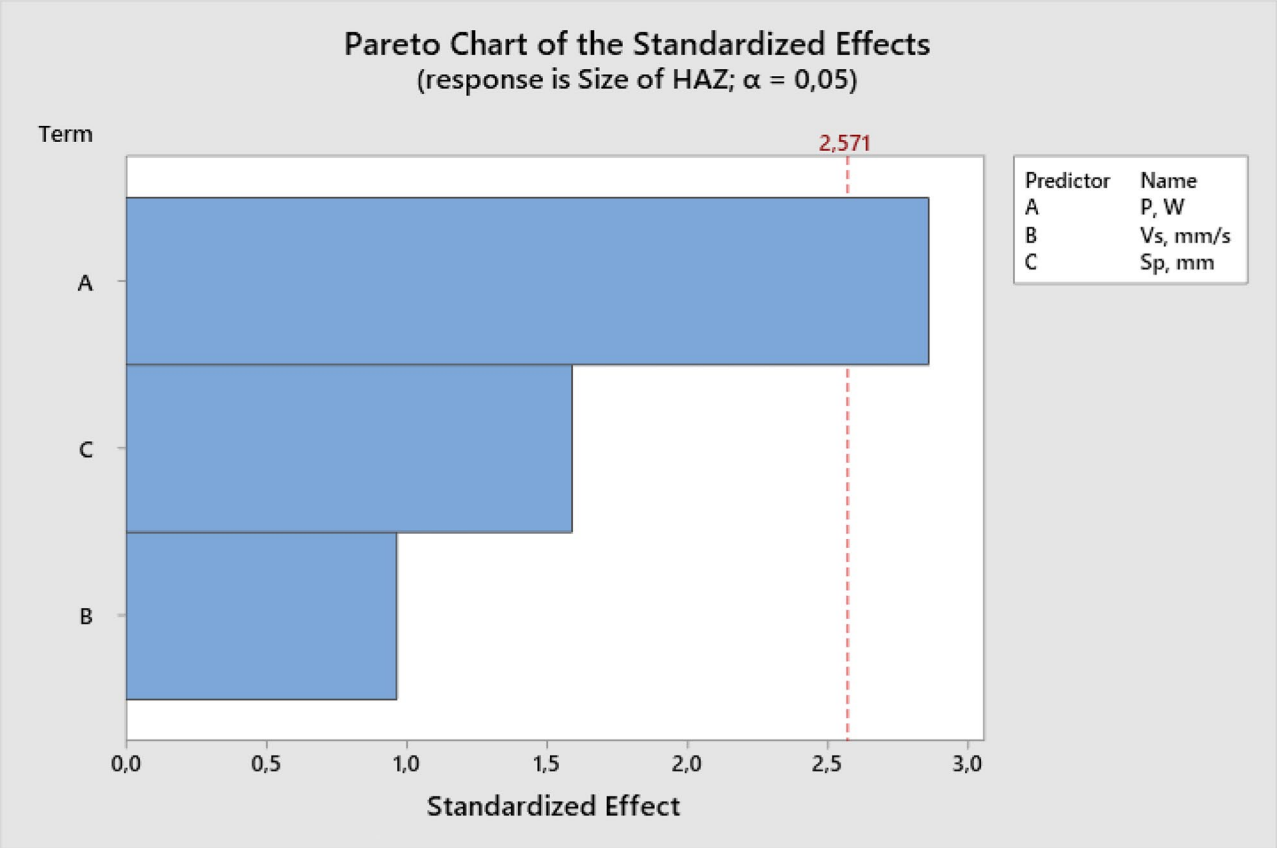

Fig. 7 Pareto chart that shows the influence of the variables on the size of the HAZ

$$S/N_i = -10\log\left(\frac{1}{n}\cdot\sum_{j=1}^{n}Y_{ij}^2\right) \quad (5)$$

Table 12 shows the S/N responses of the welding parameters for the size of the HAZ and for the percentage of dilution.

Table 13 shows a comparison between the influence of the welding variables obtained from the analysis of variance and the influence of these variables obtained from the Taguchi optimisation with the criterion 'the smaller the better'.

Table 10 Dilution values, total molten metal areas and molten base metal areas for each experiment

Experiment no.	Weld bead area (mm^2)	Molten base metal area (mm^2)	Dilution (%)
1	1.86E−05	9.72E−06	52%
2	1.25E−05	4.65E−06	21%
3	1.16E−05	3.82E−06	12%
4	1.91E−05	9.16E−06	37%
5	1.92E−05	1.00E−05	46%
6	1.57E−05	7.31E−06	47%
7	2.29E−05	1.22E−05	43%
8	1.99E−05	1.06E−05	53%
9	1.24E−05	6.11E−06	33%

The table above verifies that the power has the most significant influence; it has similar values for the ANOVA analysis and the Taguchi optimisation, both for the size of the HAZ and the dilution. However, this is not the case for Vs and Sp: the influences of these variables for both the dilution and HAZ size are inversely proportional. From this, it follows that the study of variance is not a valid method to use for the desired optimisation; it only indicates the mean influence of each of the variables on each of the measurements made (Fig. 12).

The figure above shows the optimal parameter values that can be used to obtain the minimum HAZ size. The parameter values P = 1557 W, Vs = 13 mm/s and Sp = 0 mm result in a minimum HAZ size of 0.53 mm (Fig. 13).

The figure above shows the optimal parameter values that can be used to obtain the minimum dilution. The parameter values P = 1557 W, Vs = 13 mm/s and Sp = 1 mm result in a minimum dilution value of 18%.

Methodology of Taguchi is sufficiently robust in welding processes [34]; it is not considered necessary to carry out experiments to obtain the smallest HAZ [P = 1557 W;

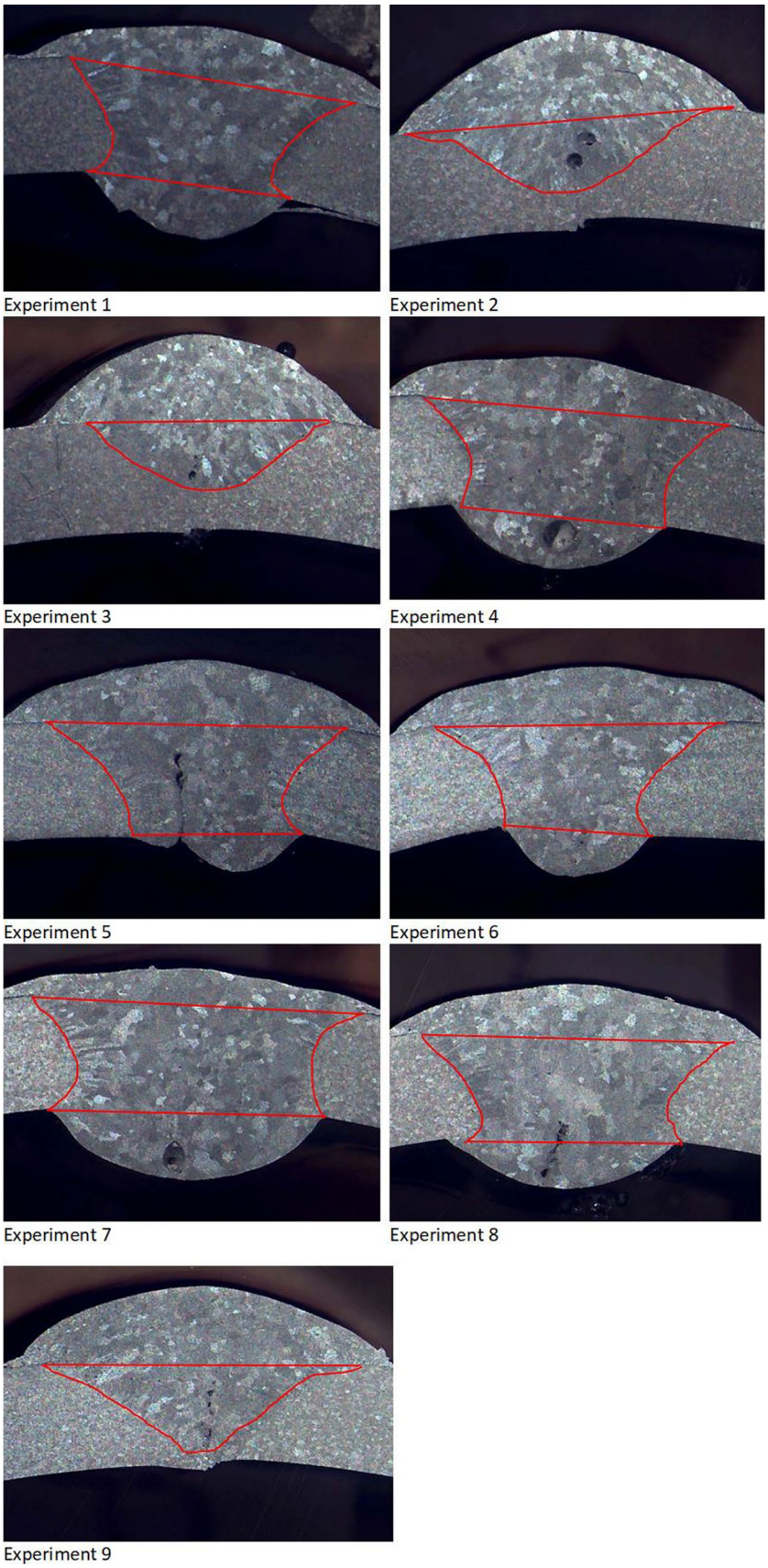

Fig. 8 Dilution measured in each of the experiments

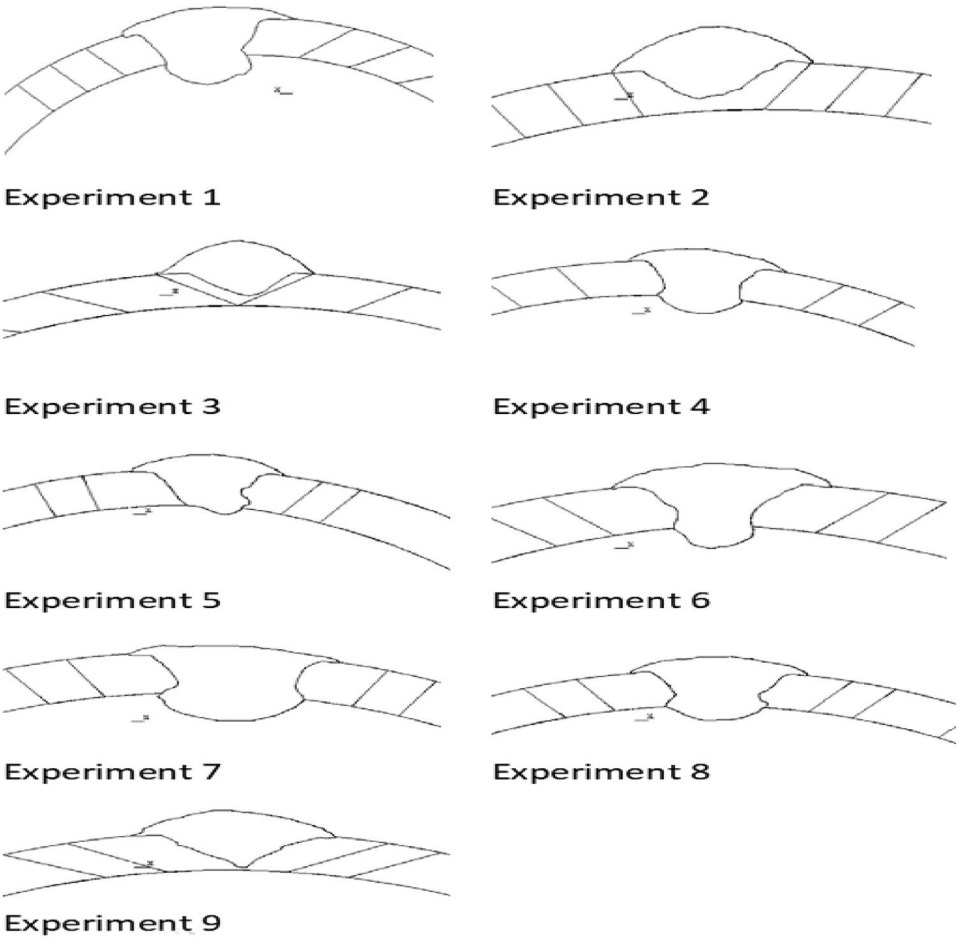

Fig. 9 Detailed representations of the weld bead and base metal for each of the experiments

Vs = 13 mm/s; Sp = 0 mm] to verify that the optimum value of the HAZ is 0.53 mm. The same happens to obtain the minimum dilution in welding [P = 1557 W; Vs = 13 mm/s; Sp = 1 mm] to verify that the optimum value of the dilution is 18%.

Table 11 Analysis of variance (ANOVA)

Source	DF	Seq SS	Seq MS	*F*-value	*P*-value
Regression	3	0.12859	0.042862	7.25	0.029
P, *W*	1	0.03719	0.037188	6.29	0.054
Vs, mm/s	1	0.02667	0.026667	4.51	0.087
Sp, mm	1	0.06473	0.064731	10.95	0.021
Error	5	0.02957	0.005914		
Total	8	0.15816			

4.2 Optimised combination of process parameters

The influences of each of the variables on the HAZ size and dilution have been analysed separately. Next, the optimal values of the three welding variables, P, Vs and Sp, needed to obtain minimal dilution and a minimal HAZ size are determined (Fig. 14).

The optimisation graph shows the effect of each input variable (columns) on the weld measurements carried out; the responses are presented in rows. The vertical red lines in the graph represent the configuration of the current value. The red numbers at the tops of the columns show the configuration of the current input variables. The horizontal blue lines and numbers represent the responses for the current factor level.

Desirability in general terms evaluates the effectiveness with which a combination of input variables satisfies the goals that have been defined for the responses. The

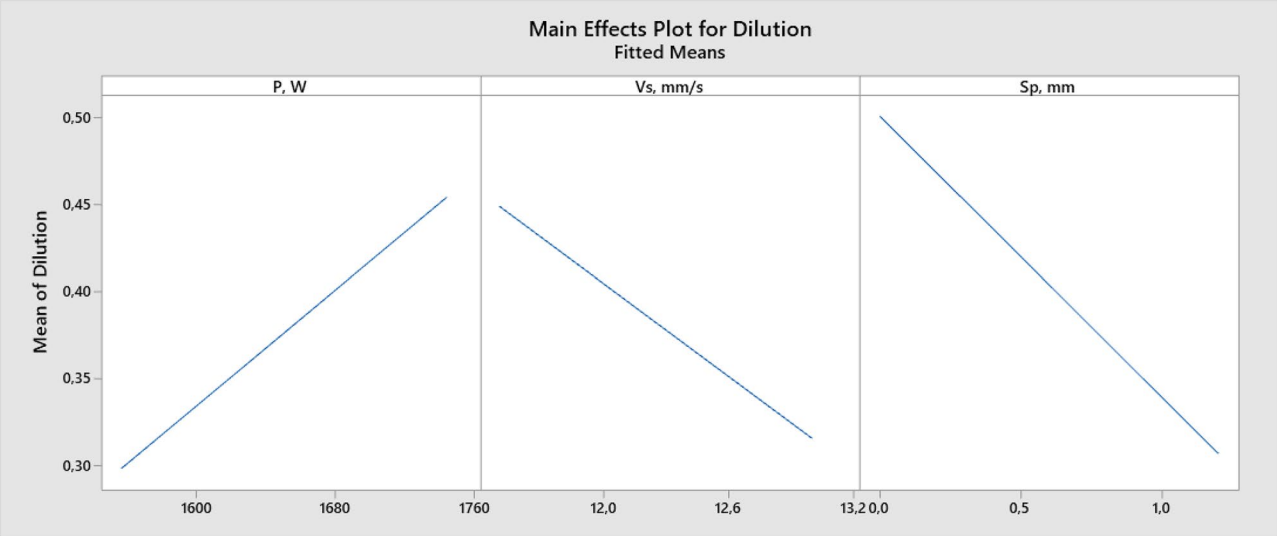

Fig. 10 Representation of the effect of each of the variables on the degree of dilution

individual desirability (d) evaluates how the configuration optimises an individual response; the composite desirability (D) evaluates how the configuration optimises a set of responses in general. Desirability has a range from 0 to 1: 1 representing the ideal situation, and 0 indicates that one or more responses are outside acceptable limits. It can be seen that the composite desirability has a value of 0.8971; thus, overall, the responses have an intermediate desirability.

The minimum value of the dilution obtained in the figure above is y = 15%, or 0.1559; it has an experimental minimum value of 12% (see Table 10). Similarly, for the HAZ, the minimum value obtained in the figure above is y = 0.71 mm, and the minimum value obtained in the experiments is 0.64 mm (see Table 8); the welding parameters used to obtain the minimum values in both cases are P = 1557 W, Vs = 13 mm/s and Sp = 1.2 mm. The combined optimization of the process parameters corresponds to experiment number 3 of Table 4.

Table 12 S/N responses of individually analysed welding parameters

Level	P (W)	*Vs* (mm/s)	*Sp* (mm)
Size of HAZ			
1	3.33395	0.93751	2.03835
2	0.38763	1.03409	2.05518
3	0.01993	1.76992	−0.35202
Delta	3.314	0.832	2.407
Rank	1	3	2
% influence	51%	13%	37%
% Dilution			
1	12.551	7.216	5.917
2	7.313	8.605	10.607
3	7.492	11.535	10.831
Delta	5.238	4.319	4.913
Rank	1	3	2
% influence	36%	30%	34%

Table 13 Influence of the ANOVA variables vs the influence of the Taguchi optimisation variables

Parameter	ANOVA	Taguchi optimisation
Size of HAZ		
P, *W*	53%	51%
Vs, mm/s	29%	13%
Sp, mm	18%	37%
Dilution		
P, *W*	32%	36%
Vs, mm/s	27%	30%
Sp, mm	42%	34%

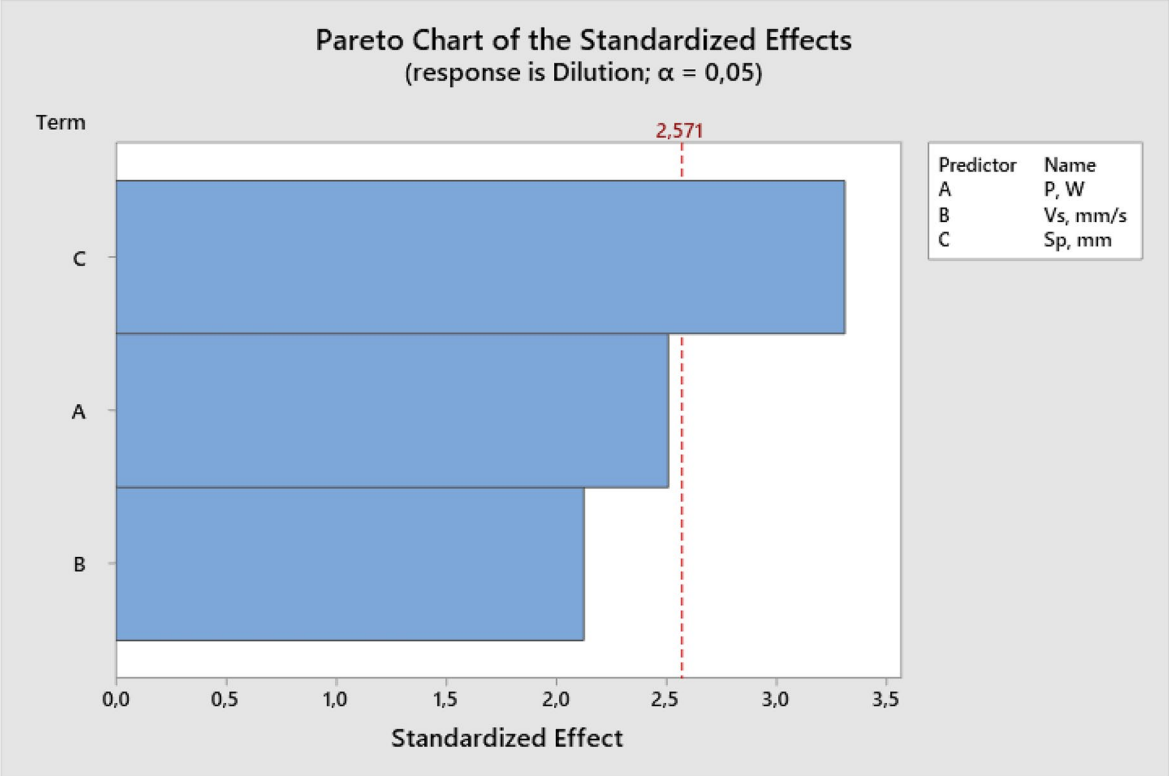

Fig. 11 Pareto diagram that shows the influence of the variables on the dilution of the base metal in the weld bead

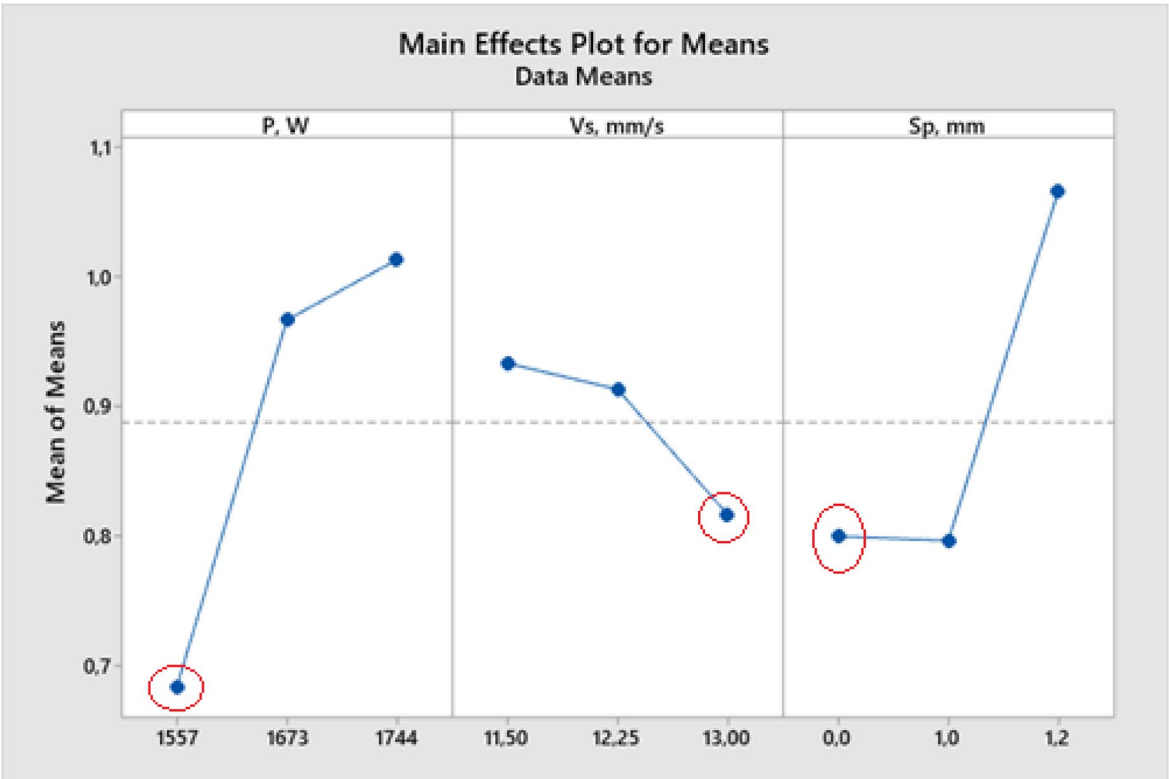

Fig. 12 Main effects of the mean values that result in a minimum HAZ size

Fig. 13 Main effects of the mean values that result in a minimum dilution

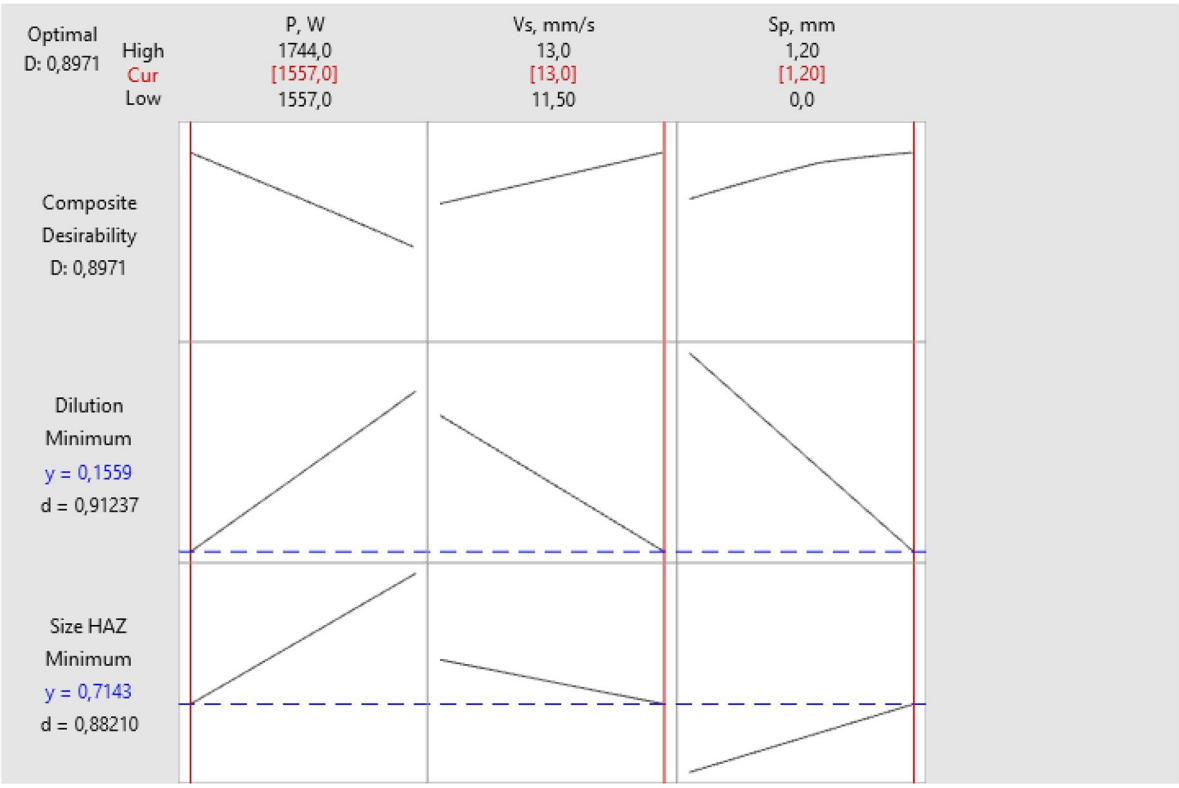

Fig. 14 Optimised combination of process parameters

5 Conclusions

(a) According to the analysis of variance carried out in Table 7, there is no relationship between the welding parameters and the grain size obtained in the experiments.
(b) In accordance with the previous conclusion, the variables were not optimised to obtain the smallest possible grain size since there is no relationship between these variables and the grain size.
(c) Regarding the size of the HAZ, the variables make the following contributions to the size of the HAZ: *P* 53%, *Vs* 18% and *Sp* 29%.
(d) Regarding the degree of dilution, the variables make the following contributions to the degree of dilution: *P* 32%, *Vs* 27% and *Sp* 42%.
(e) A Taguchi optimisation is performed to obtain the lowest possible values of both the size of the HAZ and the degree of dilution.

- To obtain the minimum size of the HAZ, the optimal welding parameters are $P = 1557$ W, $Vs = 13$ mm/s and $Sp = 0$ mm. From these values, a HAZ size of 0.53 mm is obtained.
- To obtain the minimum dilution value, the optimal welding parameters are $P = 1557$ W, $Vs = 13$ mm/s and $Sp = 1$ mm. From these values, a minimum dilution value of 18% is obtained.

(f) An optimisation of the welding parameters is carried out to obtain minimal values of both the HAZ and the degree of dilution; it produced the following values: $P = 1557$ W, $Vs = 13$ mm/s and $Sp = 1.2$ mm.
(g) The adjustment of the optimised variables is acceptable because there are high R^2 values (close to 100) and low *P*-values, which indicate that the predictive model is good.

Nomenclature GMAW: gas Gas metal arc wel; GTAW: gas Gas tungsten arcwelding; HAZ: heat Heat affected zone

Funding Open Access funding provided thanks to the CRUE-CSIC agreement with Springer Nature.

Availability of data and material The photos and images were obtained from the tests carried out in the laboratories of co-author Antonio Portoles. The Minitab statistical program is licensed by co-author Eusebio Jose Martinez Conesa.

Code availability The Minitab statistical program is licensed by co-author Eusebio Jose Martinez Conesa.

Declarations

Ethics approval Not applicable.

Consent to participate Not applicable.

Consent for publication Not applicable.

Competing interests The authors declare no competing interests.

References

1. López EA, Ramirez AJ (2015) Inhibición de la formación de compuestos intermetálicos en juntas aluminio-acero soldadas por fricción-agitación. Rev Metal 51(4):053
2. Wang Z, Oliveira JP, Zeng Z, Bu X, Peng B, Shao X (2019) Laser beam oscillating welding of 5A06 aluminum alloys: microstructure, porosity and mechanical properties. Opt Laser Technol 111:58–65
3. Ke W, Bu X, Oliveira JP, Xu W, Wang Z, Zeng Z (2021) Modeling and numerical study of keyhole-induced porosity formation in laser beam oscillating welding of 5A06 aluminum alloy. Opt Laser Technol 133:106540
4. de las Cuevas F, Aguilar C, Sevillano JG (2018) Un estudio adicional de la cinética de recristalización y crecimiento de grano del acero twip laminado en frío. Rev Metal 54(4):131
5. ASTM E112 - 13. Standard Test Methods for Determining Average Grain Size
6. ISO 643:2019. Aciers — Détermination micrographique de la grosseur de grain apparente
7. Heilbronner R (2000) Automatic grain boundary detection and grain size analysis using polarization micrographs or orientation images. J Struct Geol 22(7):969–981
8. Seward-Thompson BL, Hails JR (1973) An appraisal of the computation of statistical parameters in grain size analysis. Sedimentology 20(1):161–169
9. Oliveira JP, Crispim B, Zeng Z, Omori T, Fernandes FB, Miranda RM (2019) Microstructure and mechanical properties of gas tungsten arc welded Cu-Al-Mn shape memory alloy rods. J Mater Process Technol 271:93–100
10. Oliveira JP et al (2020) Gas tungsten arc welding of as-rolled CrMnFeCoNi high entropy alloy. Mater Des 189:108505
11. Oliveira JP, Barbosa D, Fernandes FB, Miranda RM (2016) Tungsten inert gas (TIG) welding of Ni-rich NiTi plates: functional behavior. Smart Mater Struct 25(3):03LT01
12. Delgado JA, Ambriz RR, Cuenca-Álvarez R, Alatorre N, Curiel FF (2016) Efecto del calor de aporte sobre la transformación microestructural y las propiedades mecánicas en soldadura GTAW de un acero inoxidable ferrítico 409L. Rev Metal 52(2):068

13. Meseguer-Valdenebro JL, Portolés A, Martínez-Conesa E (2017) Ciclo térmico y soldabilidad de las aleaciones de aluminio. Rev Metal 53(3):103
14. Meseguer-Valdenebro JL, Martinez-Conesa EJ, Serna J, Portoles A (2016) Influence of the welding parameters on the heat affected zone for aluminium welding. Therm Sci 20(2):643–653
15. Hunt AC, Kluken AO, Edwards GR (1994) Heat input and dilution effects in microalloyed steel weld metals. Welding Journal-New York 73:9-s
16. Roy RK (2010) A primer on the Taguchi method. Society of Manufacturing Engineers
17. Cruz-Gonzalez CE, Gala-Barron HI, Mosquera-Artamonov JD, Gamez-Cuatzin YH (2016) Effect of pulsed current in the welding process of 6AL4V in titanium with and without filler metal. Rev Metal 52(3)
18. Piccini JM, Svoboda HG (2017) Effect of tool rotational speed and penetration depth on dissimilar aluminum alloys friction stir spot welds. Rev Metal 53:1
19. Naik S, Das SR, Dhupal D, Khatua AK (2021) Analysis on surface integrity and sustainability assessment in electrical discharge machining of engineered Al-22% SiC metal matrix composite. Rev Metal 57(4):e210
20. Grillo FF et al (2020) Elaboration of synthetic slags containing marble waste and aluminum oxide used in steel desulfurization process. Rev Metal 56(3):174
21. Chinnadurai T, Vendan SA (2016) Prediction of material removal rate and surface roughness for wire electrical discharge machining of nickel using response surface methodology. Rev Metal 52(4):10–3989
22. Meseguer-Valdenebro JL, Portoles A, Matínez-Conesa E (2018) Electrical parameters optimisation on welding geometry in the 6063-T alloy using the Taguchi methods. Int J Adv Manuf Technol 98(9):2449–2460
23. Martinez-Conesa EJ, Egea JA, Miguel V, Toledo C, Meseguer-Valdenebro JL (2017) Optimization of geometric parameters in a welded joint through response surface methodology. Constr Build Mater 154:105–114
24. Meseguer-Valdenebro JL, Serna J, Portoles A, Estrems M, Miguel V, Martínez-Conesa E (2016) Experimental validation of a numerical method that predicts the size of the Heat Affected Zone. Optimization of the welding parameters by the Taguchi's method. Trans Indian Ins Met 69(3):783–791
25. Meseguer-Valdenebro JL, Portoles A, Oñoro J (2017) Numerical study of TTP curves upon welding of 6063-T5 aluminium alloy and optimization of welding process parameters by Taguchi' s method
26. Meseguer VJ, Martínez-Conesa EJ, Portolés A (2019) Numerical-experimental validation of the welding thermal cycle carried out with the MIG welding process on a 6063-T5 aluminium tubular profile. Therm Sci 00:30–30
27. Miguel V, Marín-Ortiz F, Manjabacas MC, Martínez-Conesa EJ, Martínez-Martínez A, Coello J (2015) Optimización multiobjetivo del proceso de soldeo GMAW de la aleación AA 6063-T5 basado en la penetración y en la zona afectada térmicamente. Rev Metal 51(1):037
28. Miguel V, Martínez-Conesa EJ, Segura F, Manjabacas MC, Abellán E (2012) Optimización del proceso de soldadura GMAW de uniones a tope de la aleación AA 6063-T5 basada en la metodología de superficie de respuesta y en la geometría del cordón de soldadura. Rev Metal 48(5):333–350
29. Bloem CA, Salvador MD, Amigó V, Vicente A (2007) Comportamiento a fatiga de uniones soldadas GMAW de la aleación de aluminio AA 7020. Rev Metal 43(2):111–116
30. ASM International (1998) Metal Handbook. ASM International, USA
31. Bloem CA, Salvador MD, Amigó V, Vicente A (2000) Estudio microestructural y de resistencia de uniones soldadas de la aleación AW7020 por procedimiento MIG en función de la preparación de bordes. Rev Metal 36(1):33–39
32. Mathews PG (2005) Design of Experiments with MINITAB. ASQ Quality Press Milwaukee, WI, USA
33. Prakash J, Tewari SP, Srivastava BK (2011) Shielding gas for welding of aluminium alloys by TIG/MIG welding-a review. Int J Mod Eng Res (IJMER) 1(2):690–699
34. Benyounis KY, Olabi AG (2008) Optimization of different welding processes using statistical and numerical approaches–a reference guide. Adv Eng Softw 39(6):483–496